

Transport properties in a simplified double exchange model

Phan Van-Nham and Tran Minh-Tien
*Institute of Physics, National Center for Natural Science and Technology,
P.O. Box 429, Boho, 10000 Hanoi, Vietnam.*

Transport properties of Manganite by double exchange mechanism are considered. The system is modeled by a simplified double exchange model, i.e., the Hund interaction between the spins of itinerant electrons and local spins is simplified to the Ising type. The transport quantities as the electronic conductivity, thermal conductivity, and the thermal power are calculated by the dynamical mean-field theory. It is found that the transport quantities exhibits clearly the ferromagnetic phase transition. A comparison with experiments is also presented.

PACS numbers: 71.27.+a

I. INTRODUCTION

The interest phenomena in the family of doped manganese oxides $T_{1-x}D_xMnO_3$ has been recently renewed¹⁻⁴. As doping x and temperature T are varied, these manganite show a rich variety of phases³. Particulary interesting is the doping region $0.1 < x < 0.3$, where the compounds undergo a transition from either insulating or very high resistance metallic, paramagnetic (PM) phase at high temperature to a ferromagnetic (FM) phase at low temperature. Near the transition, the resistivity of the compounds changes by a orders of magnitude. The application of a strong magnetic field substantially reduces this effect, thus giving rise to a very large negative magnetoresistance⁵. Although the physical mechanism, responsible for this behaviour has been recently the subject of much discussion and controversy. The double-exchange (DE) mechanism⁴ still provides a well established starting point. The DE model was proposed by Zenner⁴ who considered the explicit movement of electrons schematically written as $Mn_{1\uparrow}^{3+}O_{2\uparrow,3\downarrow}Mn^{4+} \rightarrow Mn^{4+}O_{1\uparrow,3\downarrow}Mn_{2\uparrow}^{3+}$ where 1,2 and 3 label electrons that belong either to the oxygen between manganese or to the e_g level of the Mn ions. In this process, there are two simultaneous motions involving electron moving from the oxygen to the Mn^{4+} ions and other electron from the Mn^{3+} to the oxygen². In the DE process the motion of the itinerant electron favors the ferromagnetic ordering of the local spins and, vive versa, the presence of ferromagnetic order facilitates the motion of the itinerant electron. Hence, only the z-component part of the Hund interaction between the local spins and spins of the itinerant electron plays an essential role in the DE. In this paper we study the transport properties by the simplified DE (SDE) where only z-component part of Hund interaction is incorporated. The transport quantities such as the dc-conductivity, thermal conductivity and thermal power are calculated by Dynamical mean-field theory (DMFT). The DMFT has been extensively used for inverstigating strongly correlated electron systems. It is based on the fact that the self-energy depends only on frequency in the infinite dimension limit. Using the DMFT these

transport quanities can be expressed via the spectral function.

We find that the SDE captures main features of the transport properties of manganites. These results indicate that the DE process in manganites can be studied by the SDE model which is much simpler than the full version of the DE model. This provides a starting point toward to complex including various variations to the DE mechanism such as the randomness, charge or orbital ordering.

The poster is organized as follows. In section II we present the SDE model and formulas for dc-conductivity, thermal conductivity and thermal power. In section III we provide the application DMFT in SDE model. Next section we present numerical results for the thermal transport illustrating the different contributions of Hund coupling and concentration of itinerant electrons. Conclusions are presented in section IV.

II. TRANSPORT COEFFICIENTS IN SDE MODEL

The Hamiltonian of the SDE model is described as follows

$$H = - \sum_{\langle ij \rangle, \sigma} t_{ij} c_{i\sigma}^\dagger c_{j\sigma} - \mu \sum_{i, \sigma} c_{i\sigma}^\dagger c_{i\sigma} - 2J_H \sum_i S_i^z s_i^z, \quad (1)$$

where $c_{i\sigma}^\dagger$ ($c_{i\sigma}$) is the creation (annihilation) operator for an electron itinerant at site i with spin σ . The first term includes the hopping only between the nearest neighbour sites ion, t_{ij} is the hopping integral and is scaled with the spatial dimension d and to have a finite result in the limit $d \rightarrow \infty$.⁶

$$t_{ij} = \frac{t^*}{2\sqrt{d}}$$

and we take $t^* = 1$ as the unit of energy. In the limit $d \rightarrow \infty$, the bare density of states of the itinerant electron becomes $\rho(\epsilon) = \frac{1}{\sqrt{\pi}} e^{-\epsilon^2}$ for a hypercubic lattice. μ is chemical potential. The last term is the Hund

coupling between the spins of itinerant s_i^z electron and local spin S_i^z . In this model, only z component (Ising type) is concerned. Transport coefficient are calculated with in a Kubo-Greenword formalism, in which the dc-conductivity σ , thermal power S and the thermal conductivity κ can be determined from relavant correlation function of the current operator¹⁰. We define three transport coefficients as L^{11} , $L^{12} = L^{21}$ and L^{22} , we have

$$\sigma = \frac{e^2}{T} L^{11} \quad (2)$$

$$S = -\frac{1}{eT} \frac{L^{12}}{L^{11}} \quad (3)$$

$$\kappa = L^{22} - \frac{(L^{12})^2}{L^{11}} \quad (4)$$

where the transport coefficients are found from the analytic continuation of the relevant "polarization operator" at zero frequency¹⁰, that mean

$$L^{ij} = \lim_{\nu \rightarrow 0} TIm \frac{L^{ij}(\nu)}{\nu} \quad (5)$$

where $L^{ij}(\nu)$ can be calculated from the correlation functions

$$\bar{L}^{11}(i\nu_n) = \int_0^\beta d\tau e^{i\nu_n \tau} \langle T_\tau \mathbf{j}(\tau) \mathbf{j}(0) \rangle \quad (6)$$

$$\bar{L}^{12}(i\nu_n) = \int_0^\beta d\tau e^{i\nu_n \tau} \langle T_\tau \mathbf{j}(\tau) \mathbf{j}_Q(0) \rangle \quad (7)$$

$$\bar{L}^{22}(i\nu_n) = \int_0^\beta d\tau e^{i\nu_n \tau} \langle T_\tau \mathbf{j}_Q(\tau) \mathbf{j}_Q(0) \rangle \quad (8)$$

after replace $i\nu_n$ by $\nu + i\delta$ ($\delta \rightarrow 0^+$), here \mathbf{j} and \mathbf{j}_Q are particle-current operator and heat-current operator, respectively. The particle-current operator is defined by the commutator of the Hamiltonian with the polarization operator $\sum_i \mathbf{R}_i n_i$ ¹⁰, with our model we have.

$$\mathbf{j} = \sum_{\mathbf{q}} v_{\mathbf{q}} c_{\mathbf{q}\sigma}^\dagger c_{\mathbf{q}\sigma} \quad (9)$$

where the velocity operator is $v_{\mathbf{q}} = \nabla_{\mathbf{q}} \epsilon(\mathbf{q})$ and $c_{\mathbf{q}\sigma}^\dagger$ is Fourier transform of the $c_{i\sigma}^\dagger$: $c_{\mathbf{q}\sigma}^\dagger = \frac{1}{N} \sum_{\sigma} e^{i\mathbf{q}\mathbf{R}_i} c_{i\sigma}^\dagger$ and the energy-current is defined by the commutator of the Hamiltonian with the energy polarization operator $\sum_i \mathbf{R}_i h_i$ (where $H = \sum_i h_i$), with this defined a heat-current operator is

$$\mathbf{j}_Q = \mathbf{j}_E - \mu \mathbf{j} = \sum_{\mathbf{q}\sigma} \mathbf{v}_{\mathbf{q}} [\epsilon(\mathbf{q}) - \mu] c_{\mathbf{q}\sigma}^\dagger c_{\mathbf{q}\sigma}$$

$$- \frac{1}{2} \sum_{\mathbf{q}, \mathbf{q}'} J_H \sigma S(\mathbf{q} - \mathbf{q}') (\mathbf{v}_{\mathbf{q}'} + \mathbf{v}_{\mathbf{q}}) c_{\mathbf{q}\sigma}^\dagger c_{\mathbf{q}\sigma} \quad (10)$$

where $S(\mathbf{q} - \mathbf{q}') = \frac{1}{N} \sum_i S_i^z e^{-i(\mathbf{q}-\mathbf{q}') \cdot \mathbf{R}_i}$. The important relations between the heat-current and the particle-current operator are described fully bellow. Substubting \mathbf{j} and \mathbf{j}_Q from (9) and (10) into (6)(7) and (8), the transport coefficients are easy calculated in the infinite dimensional hypercubic.

$$L^{11} = T \sum_{\sigma} \int d\epsilon \rho(\epsilon) \int d\omega \left(-\frac{\partial f(\omega)}{\partial \omega} \right) A_{\sigma}^2(\epsilon, \omega) \quad (11)$$

$$L^{12} = T \sum_{\sigma} \int d\epsilon \rho(\epsilon) \int d\omega \left(-\frac{\partial f(\omega)}{\partial \omega} \right) A_{\sigma}^2(\epsilon, \omega) \omega \quad (12)$$

and

$$L^{22} = T \sum_{\sigma} \int d\epsilon \rho(\epsilon) \int d\omega \left(-\frac{\partial f(\omega)}{\partial \omega} \right) A_{\sigma}^2(\epsilon, \omega) \omega^2 \quad (13)$$

Above results (11), (12) and (13) appears $A_{\sigma}(\epsilon, \omega)$ as spectrum function of its Green function

$$A_{\sigma}(\epsilon, \omega) = -\frac{1}{\pi} Im G_{\sigma}(\epsilon, \omega) \quad (14)$$

That ideal lead us to calculate Green function for each electron with spin σ . In this poster, Green function were found for the SDE by DMF theory approximation.

III. APPLICATION DMF THEORY IN SDE MODEL

We solve the SDE model (1) by the DMFT. The DMFT is based on the infinite dimension limit. In the infinite dimension limit the self-energy is pure local and does not depend on momentum. The Green function of the itinerant electrons with spin σ satisfies the Dyson equation

$$G_{\sigma}(\mathbf{k}, i\omega_n) = \frac{1}{i\omega_n - \epsilon(\mathbf{k}) + \mu - \Sigma_{\sigma}(i\omega_n)}, \quad (15)$$

So we have local (single-site) Green function

$$G_{L\sigma}(i\omega_n) = \frac{1}{N} \sum_{\mathbf{k}} G_{\sigma}(\mathbf{k}, i\omega_n) = \int d\epsilon \rho(\epsilon) \frac{1}{i\omega_n - \epsilon(\mathbf{k}) + \mu - \Sigma_{\sigma}(i\omega_n)}, \quad (16)$$

where $\omega_n = \pi T(2n + 1)$ is the Matsubara frequency, $\epsilon(\mathbf{k}) = -2t \sum_{\alpha} \cos(k_{\alpha})$ is the dispersion of the free itinerant electrons on a hypercubic lattice, $\Sigma_{\sigma}(i\omega_n)$ is the self-energy. The self-energy is determined by solving an effective single-site problem. The effective action for this problem is.

$$S_{eff} = - \int d\tau \int d\tau' \sum_{\sigma} c_{\sigma}^{\dagger}(\tau) \mathcal{G}_{\sigma}^{-1}(\tau - \tau') c_{\sigma}(\tau') + 2J_H \int d\tau S^z \sum_{\sigma} \sigma c_{\sigma}^{\dagger}(\tau) c_{\sigma}(\tau) \quad (17)$$

where $\mathcal{G}_{\sigma}(\tau - \tau')$ is the Green function of the effective medium $\mathcal{G}_{\sigma}(i\omega_n)$ in the time representation.

The local Green function of the effective single-site problem is solely determined by the partition function. It can be calculated by the equation.

$$G_{\sigma}(i\omega_n) = \frac{\partial \mathcal{Z}_{eff}}{\partial \mathcal{G}_{\sigma}^{-1}(i\omega_n)} \quad (18)$$

where \mathcal{Z}_{eff} is the partition function

In addition to (16), the local Green function $G_{L\sigma}(i\omega_n)$ can be considered as the Green function of a single-site problem with a certain effective bare Green function $\mathcal{G}_{\sigma}(i\omega_n)$ and with the same self-energy $\Sigma_{\sigma}(i\omega_n)$, so that we can write

$$G_{L\sigma}(i\omega_n) = \frac{1}{\mathcal{G}_{\sigma}^{-1}(i\omega_n) - \Sigma_{\sigma}(i\omega_n)} \quad (19)$$

From (16)(18) and (19) we have self-consistently equations, which the self-energy and the Green function are determined. Within the effective single-site problem, the partition function becomes

$$\mathcal{Z}_{eff} = Tr \int Dc_{\sigma}^{\dagger} Dc_{\sigma} e^{-S_{eff}} \quad (20)$$

where the trace is taken over S_z . This partition function can be calculated exactly, this similar to DMFT solving the FK model⁶ we obtain

$$\mathcal{Z}_{eff} = \sum_m e^{-\beta \int d\omega f(\omega) \frac{1}{\pi} Im \sum_{\sigma,n} \ln(\mathcal{G}_{\sigma}^{-1}(\omega) - J_H \sigma m)} \quad (21)$$

where $m = -\frac{3}{2}, -\frac{3}{2} + 1, \dots, \frac{3}{2}$ are projections of S on z axis.

Using Eq.(18) we obtain the local Green function

$$G_{L\sigma}(i\omega_n) = \sum_m \frac{w_m}{\mathcal{G}_{\sigma}^{-1} - J_H \sigma m} \quad (22)$$

where

$$w_m = \frac{1}{\mathcal{Z}_{eff}} e^{-\beta \int d\omega f(\omega) \frac{1}{\pi} Im \sum_{\sigma,n} \ln(\mathcal{G}_{\sigma}^{-1}(\omega) - J_H \sigma m)} \quad (23)$$

IV. NUMERICAL RESULTS

We present the DMFT results for two cases: $n = 1.0$ (half filling) and $n = 0.5$ (quarter filling) where $n = -\frac{1}{\pi} T \sum_{\sigma,n} Im \mathcal{G}_{\sigma}(i\omega_n)$ with two values of $J = 2J_H$ ($J = 2$ and $J = 4$). The algorithm for determining the Green function is as follows. (i) Begin with the self-energies in each spin ($\Sigma_{\uparrow} = 0.5$ and $\Sigma_{\downarrow} = 0.0$). (ii) Then (16) is used to find the local Green function. (iii) Substituting Σ_{σ} in (i) and G_{σ} were calculated in (ii) to (18) we have the effective medium \mathcal{G}_{σ} . (iv) Put \mathcal{G}_{σ} into (19) G_{σ} are determined. (v) From these G_{σ} and \mathcal{G}_{σ} were determined in (iii) and together with (18) two new Σ_{σ} are present. Go back to step (ii) and repeat the iteration until convergence is reached. In all our calculations, the relative error for the Green function of less than 10^{-7} is used to stop iteration loop. Our results of transport properties in SDE is expressed follow.

Fig.1 shows the temperature dependence of the re-

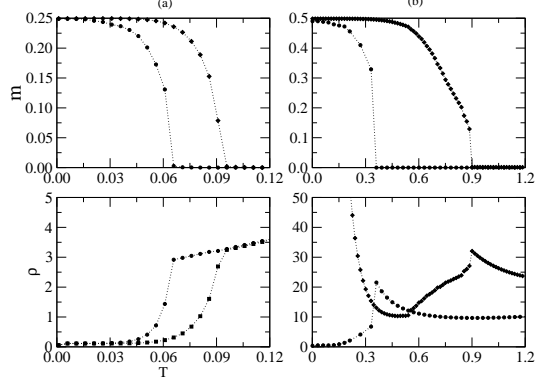


FIG. 1: Temperature dependence of the resistivity ρ and magnetization m for different electron fillings: (a) ($n = 0.5$), (b) ($n = 1.0$). The line with filled circles denotes $J = 2$ and the line with diamonds denotes $J = 4$

sistivity for different electron fillings n in two different Hund coupling constant J . Fig.1(a) provides a decrease in the resistivity when the magnetization increases in the case $n = 0.5$. Indeed, in the limit $T \rightarrow 0$, or $m \rightarrow 0.25$, the density of states (DOS) of spin-up electron $A_{\uparrow}(\epsilon, \omega) = \delta(\omega + \mu - \epsilon)$ is maximum at $\omega = 0$, that mean conduction electron-subsystem becomes a free electron gas of spin-up electron. Increasing temperature, Fig. 2 shows that, DOS of spin-up electron is still maximum at $\omega = 0$ and system in ferromagnetic-metallic phase with dependence of resistivity on temperature is quadratic. On the other hand, in high-temperature paramagnetic phase, $m = 0$ as DOS of spin-up electrons and spin-down electrons is coincides with each other but their values at $\omega = 0$ are not equal zero so system in paramagnetic-metal phase.

The sharp decreases of resistivity at $T < T_c$ for all J

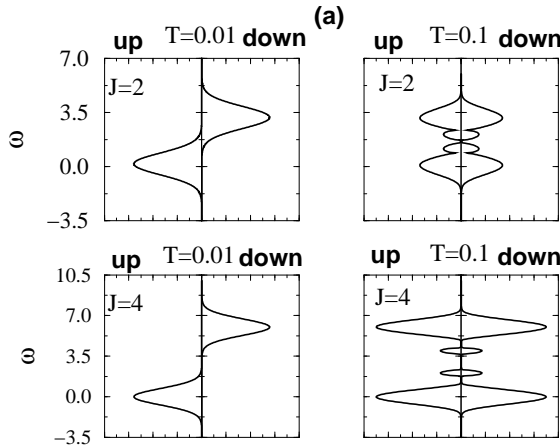


FIG. 2: Density of states (DOS) $A_\sigma(\omega)$ as a function of frequency for different temperature T in ($n = 0.5$) with different J : left for $J = 2$, right for $J = 4$. Label 1 and 2 denotes the DOS for spin-up and spin-down electron, respectively.

is caused by rapid increases of the magnetization m . This discontinuity in the slope $d\rho/dT$ at $T = T_c$ is consequence of the dynamical mean field approach. Incorporation of spatial spin fluctuations¹³ will smooth out the temperature dependence of the resistivity in the vicinity of T_c , but this is beyond DMFT.

Increasing J constant, the shape of resistivity vs temper-

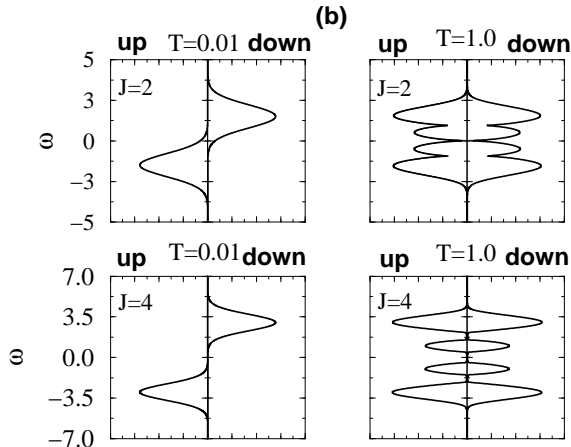


FIG. 3: Density of states (DOS) $A_\sigma(\omega)$ as a function of frequency for different temperature T in ($n = 1.0$) with different J : left for $J = 2$, right for $J = 4$. Label 1 and 2 denotes the DOS for spin-up and spin-down electron, respectively.

ature has a little modification but the Curie-temperature increases. This analysis is in qualitative agreement with the calculations in⁹ with disorder strengths $\Delta = 0$ and the experimental data on manganites.

As concentration of itinerant electron increases to $n = 1$,

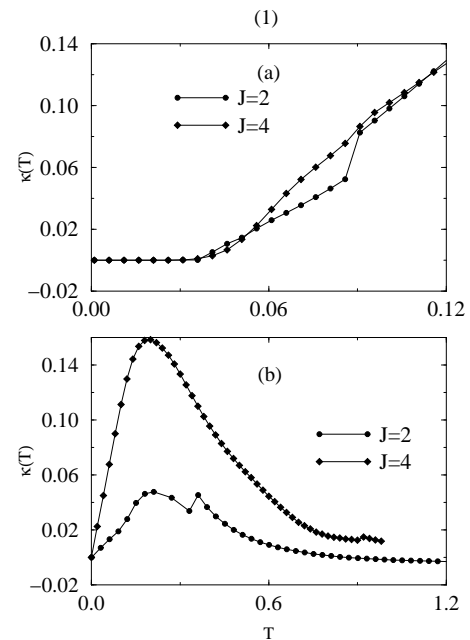


FIG. 4: Temperature dependence of the thermal conductivity κ for different electron fillings: (a) ($n = 0.5$), (b) $n = 1.0$. The line with filled circles denotes $J = 2$ and the line with diamonds denotes $J = 4$

Fig. 1(b) shows more puzzle dependence of function $\rho(T)$ on Hund coupling constant than $n = 0.5$ case. Indeed, when J is small ($J = 2$), Fig. 3 shows that, at low temperature, the DOS of spin-up electrons and spin-down electrons overlap each other, that mean, there is only one band energy so the dependence of resistivity on temperature is in the metallic phase. But when temperature increases, in paramagnetic phase, DOS have a gap at $\omega = 0$, that mean system in insulator phase with the negative $d\rho/dT$ above T_c . When J is larger $J = 4$, system displays insulating behaviour everywhere as Fig. 3(b) shows in all temperature, there are a gap at $\omega = 0$, except just below the Curie point, where the rapid increases in the magnetization can cause the resistance to drop over a small temperature range before it turns around and increases again. This occurs in the transition from the paramagnetic insulator to the ferromagnetic-insulator phase because the charge gap in the ferromagnetic-insulator is smaller than the charge gap in the paramagnetic-insulator. Those sharp in Fig. 1(b) will generically be smoothed out by spatial fluctuations.

Now, we examine the thermal properties of our system including the thermal power $S(T)$ and the thermal conductivity $\kappa(T)$ which are shown in Fig. 4 and Fig. 5. The thermal conductivity behaves as expected with the behaviors of resistivity. In $n = 0.5$ case, system in metallic phase in all temperature so $\kappa(T)$ increases everywhere in temperature range, and when $n = 1$ the ther-

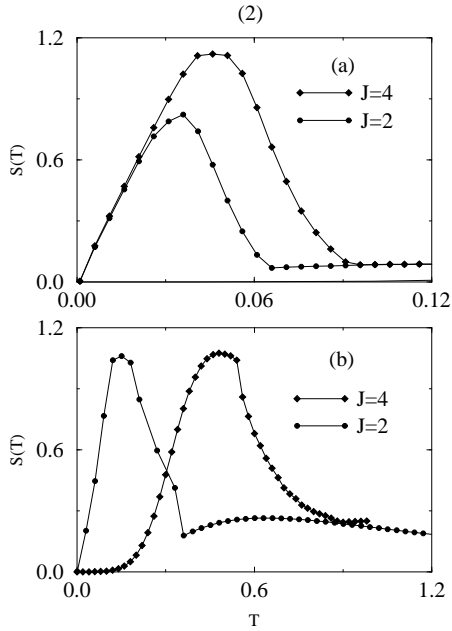


FIG. 5: Temperature dependence of the thermal power S for different electron fillings: (a) ($n = 0.5$), (b) $n = 1.0$. The line with filled circles denotes $J = 2$ and the line with diamonds denotes $J = 4$

mal conductivity has a sharp at T_c temperature and decreases in insulator phase. At low temperature, thermal conductivity has a peak and then reach to zero when $T \rightarrow 0$. This calculations agree with the calculated electrical thermal conductivity from electrical resistiv-

ity in a $La_{0.67}(Ca, Pb)_{0.33}MnO_3$ single crystal using the Wiedmann-Franz law¹.

The thermal power behaves as expected with a linear decreases to zero at low temperature which agrees with the behaviours of $S(T)$ vs temperature for a mixed $Pb - Ca$ doped sample¹. At T_c temperature, the slope of the thermal power dS/dT has a discontinuity, but $S(T)$ does not change sign in our model, that because in our model the itinerant-electron subsystem is not a Fermi liquid and the derivative of the chemical potential $d\mu/dT$ does not change sign at $T = T_c$ (does not agree with prediction in¹²)

V. CONCLUSIONS

In this poster, we have considered the transport properties in SDE model by employing DMF theory. With DMF theory we had three self-consistent equations which is easy calculated by numerical. Although the manganites are too complicated a system to be described completely by this simple model, we still arrive at some useful conclusions: The first in this model the various phases and picture of transition phase of system exit. The second, qualitative behaviours of $S(T)$ and $\kappa(T)$ agree with experiment data, special at low temperature. So with this simplified model qualitative transport properties of DE are presented. But as we have said, above results only are qualitative conclusion. Nevertheless, basic transport properties of Manganite are presented and DMF theory cooperating with DE succeed in investigating Manganite compounds.

¹ M. B. Salamon and M. Jaime, Rev. Mod. Phys. **73**, 583 (2001).
² E. Dagotto, T. Hotta, and A. Moreo, Physics Reports **344**, 1 (2001).
³ Y. A Izyumov and Y. N. Skryabin, " Double exchange model and the unique properties of the manganites" , Physics- Uspekhi **44**, 109 (2001).
⁴ J. M. D. Coery, M. Viret, and S.Von Molnar, " Mixed-valence manganites", Advances in Physics. **48**, 167 (1995).
⁵ D. M. Edwards, ACM. Green, and K. Kubo, cond-mat/9901133
⁶ A. Georges, G. Kotliar, W. Krauth, and M. J. Rozenberg, " Dynamical mean field theory of strongly correlated fermion systems and the limit of infinite dimensions", Rev. Mod. Phys. **68**, 13 (1996).
⁷ E. Dagotto, S. Yunoki, A. L. Malvezzi, A. Moreo, J. Hu, S. Capponi, D. Poilblanc, and Furukawa, cond-mat/9709029
⁸ N. Furukawa, Proc. Conference on physics of Manganites (1998), cond-mat/9812066.
⁹ B. M. Letfulov and J. H. Freericks, Phys. Rev. B **64**, 174409 (2001).
¹⁰ G. D. Mahan, " Many-Particle Physics", 2nd edition, Plenum Press (1990).
¹¹ J. K. Freericks and V. Zlatic, cond-mat/0108500.
¹² D. P. Arovas, G. Gomez-Santos, and F. Guinea, Phys. Rev. B **59**, 13 569 (1999).
¹³ S. Ishizaka and S. Ishizara, Phys. Rev. B **59**, R 8375 (1999).
¹⁴ T. Pruschke, D. L. Cox, and M. Jarrell, Phys. Rev. B **47** 3553 (1993).